ドパミンアゴニスト徐放性製剤の使い方とその治療戦略	長谷川一子，下村登喜夫，高橋一司，坪井義夫	Pahrma Medica	2014	国内
パーキンソン病	長谷川一子	ENTONI	2014-4	国内
脊髄小脳変性症の症状と対応	長谷川一子	難病と在宅ケア	2014-5	国内
進行期の患者さんに伝えたいパーキンソン病の治療と自己管理の基本	長谷川一子	マックス	2014	国内
首下がり症候群：遺伝性脊髄小脳変性症に伴う首沙汰離症候群ーMachado-Joseph病など	長谷川一子	神経内科	2014-7	国内
Huntington病の症候・病態から新たな薬物療法まで	長谷川一子	神経治療学	2014-9	国内
パーキンソン病とパーキンソン病関連疾患	長谷川一子	Brain Nursing	2014-12	国内
ハンチントン病	長谷川一子	Brain Nursing	2014-12	国内
パーキンソン病の振戦	堀内恵美子，長谷川一子	治療	2014-11	国内
ハンチントン病	長谷川一子	今日の治療指針	2014	国内
ジストニアの定義と分類	長谷川一子	神経症候群（日本臨床）	2014	国内
ドパ反応性ジストニア，芳香族L-アミノ酸脱炭酸酵素欠損症，セピアプテリン還元酵素欠損症，チロシン水酸化酵素欠損症，ピルボイルーテトラヒドロビオプテリン欠損症	長谷川一子	神経症候群（日本臨床）	2014	国内
Neurodegeneration with brainiron accumulation-1 NBIA1.	長谷川一子	神経症候群（日本臨床）	2014	国内
Novel neuronal cytoplasmic inclusions in a patient carrying SCA8 expansion mutation.	Yokoyama T, Ishiyama M, Hasegawa K, Uchihara T, Yagishita.	Neuropathology	2014	国内

Late onset GM2 gangliosidosis presenting with motor neuron disease: an autopsy case.	Yokoyama T, Nakamura S, Horiuchi E, Ishiyama M, Kawashima R, Nakamura K, Hasegawa K, Yagishita S.	Neuropathology	2014	国内
Official Japanese Version of the International Parkinson and Movement Disorder Society-Unified Parkinson's Disease Rating Scale: Validation Against the Original English Version.	Kenichi Kashihara, Tomoyoshi Kondo, Yoshikuni Mizuno, Seiji Kikuchi, Sadako Kuno, Kazuko Hasegawa, Nobutaka Hattori, Hideki Mochizuki, Hideo Mori, Miho Murata Masahiro Nomoto, Ryosuke Takahashi, Atsushi Takeda, Yoshio Tsuboi, Yoshikazu Ugawa, Mitsutoshi Yamanmoto, Fusako Yokochi, Fumihito Yoshii, Glenn T. Stebbins, Barbara C. Tilley, Sheng Luo, Lu Wang, Nancy R. LaPelle, Christopher G. Goetz, MDS-UPDRS Japanese Validation Study Group.	Mov Disord	2014	国外

Clinical correlations with Lewy body pathology in *LRRK2*-related Parkinson's disease.	LV Kalia[1], AE Lang[1], L Hazrati[1], S Fujioka[2], ZK Wszolek[2], DW Dickson[2], OA Ross[2], V-M Van Deerlin[3], JQ Trojanowski[3], HI Hurtig[3], RN Alcalay[4], KS Marder[4], LN Clark[4], C Gaig[5], E Tolosa[5], J Ruiz-Martinez[6], J Marti Masso[6], I Ferrer[7], A Lopez de Munain[6], SM Goldman[8], B Schüle[8], J Langston[8], J Aasly[9], MT Giordana[10], V Bonifati[11], A Puschmann[12], M Canesi[13], G Pezzoli[13], A Maues de Paula[14], K Hasegawa[15], C Duyckaerts[16], A Brice[16], C Marras[1]	JAMA neurol	2015. 1	国外
Possible involvement of iron-induced oxidative insults in neurodegeneration.	Asano T, Koike M, Sakata S, Takeda Y, Nakagawa T, Hatano T, Ohashi S, Funayama M, Yoshimi K, Asanuma M, Toyokuni S, Mochizuki H, Uchiyama Y, Hattori N, Iwai K.	Neurosci Lett	2014 Dec 27	国外
Rotigotine vs ropinirole in advanced stage Parkinson's disease: A double-blind study.	Mizuno Y, Nomoto M, Hasegawa K, Hatttori N, Kondo T, Murata M, Takeuchi M, Takahashi M, Tomida T; on behalf of the Rotigotine Trial Group.	Parkinsonism Relat Disord	2014	国際

Transdermal rotigotine in advanced Parkinson's disease: a randomized, double-blind, placebo-controlled trial.	Nomoto M, Mizuno Y, Kondo T, Hasegawa K, Murata M, Takeuchi M, Ikeda J, Tomida T, Hattori N.	J Neurol	2014	国際
Molecular epidemiology and clinical spectrum of hereditary spastic paraplegia in the Japanese population based on comprehensive mutational analyses.	Ishiura H, Takahashi Y, Hayashi T, Saito K, Furuya H, Watanabe M, Murata M, Suzuki M, Sugiura A, Sawai S, Shibuya K, Ueda N, Ichikawa Y, Kanazawa I, Goto J, Tsuji S.	J Hum Genet	2014	国際

（注１）発表者氏名は、連名による発表の場合には、筆頭者を先頭にして全員を記載すること。
（注２）本様式はexcel形式にて作成し、甲が求める場合は別途電子データを納入すること。

ⅠⅤ. 研究成果の刊行物･別刷

CHCHD2 mutations in autosomal dominant late-onset Parkinson's disease: a genome-wide linkage and sequencing study

Manabu Funayama, Kenji Ohe, Taku Amo, Norihiko Furuya, Junji Yamaguchi, Shinji Saiki, Yuanzhe Li, Kotaro Ogaki, Maya Ando, Hiroyo Yoshino, Hiroyuki Tomiyama, Kenya Nishioka, Kazuko Hasegawa, Hidemoto Saiki, Wataru Satake, Kaoru Mogushi, Ryogen Sasaki, Yasumasa Kokubo, Shigeki Kuzuhara, Tatsushi Toda, Yoshikuni Mizuno, Yasuo Uchiyama, Kinji Ohno, Nobutaka Hattori

Lancet Neurol 2015; 14: 274–82
Published Online February 4, 2015
http://dx.doi.org/10.1016/S1474-4422(14)70266-2
See Comment page 238

Research Institute for Diseases of Old Age (M Funayama PhD, H Yoshino PhD, Prof Y Uchiyama MD, Prof N Hattori MD) and Department of Research and Therapeutics for Movement Disorders (N Furuya PhD), Graduate School of Medicine, Juntendo University, Tokyo, Japan; Division of Neurogenetics, Center for Neurological Diseases and Cancer, Nagoya University Graduate School of Medicine, Nagoya, Japan (K Ohe MD, Prof K Ohno MD); Training Program of Leaders for Integrated Medical System for Fruitful Healthy-Longevity Society (LIMS), Kyoto University Graduate School of Medicine, Kyoto, Japan (K Ohe); Department of Applied Chemistry, National Defense Academy, Yokosuka, Japan (T Amo PhD); Department of Cellular and Molecular Neuropathology (J Yamaguchi MSc, Prof Y Uchiyama), Department of Neurology (M Funayama, N Furuya, S Saiki MD, Y Li MD, K Ogaki MD, M Ando MD, H Tomiyama MD, K Nishioka MD, Prof Y Mizuno MD, Prof N Hattori), and Center for Genomic and Regenerative Medicine (K Mogushi PhD), Juntendo University School of Medicine, Tokyo, Japan; Department of Neurology, National Hospital Organization, Sagamihara National Hospital, Sagamihara, Japan (K Hasegawa MD); Department of Neurology, Tazuke Kofukai Medical Research Institute and Kitano Hospital, Osaka, Japan

Summary

Background Identification of causative genes in mendelian forms of Parkinson's disease is valuable for understanding the cause of the disease. We did genetic studies in a Japanese family with autosomal dominant Parkinson's disease to identify novel causative genes.

Methods We did a genome-wide linkage analysis on eight affected and five unaffected individuals from a family with autosomal dominant Parkinson's disease (family A). Subsequently, we did exome sequencing on three patients and whole-genome sequencing on one patient in family A. Variants were validated by Sanger sequencing in samples from patients with autosomal dominant Parkinson's disease, patients with sporadic Parkinson's disease, and controls. Participants were identified from the DNA bank of the Comprehensive Genetic Study on Parkinson's Disease and Related Disorders (Juntendo University School of Medicine, Tokyo, Japan) and were classified according to clinical information obtained by neurologists. Splicing abnormalities of *CHCHD2* mutants were analysed in SH-SY5Y cells. We used the Fisher's exact test to calculate the significance of allele frequencies between patients with sporadic Parkinson's disease and unaffected controls, and we calculated odds ratios and 95% CIs of minor alleles.

Findings We identified a missense mutation (*CHCHD2*, 182C>T, Thr61Ile) in family A by next-generation sequencing. We obtained samples from a further 340 index patients with autosomal dominant Parkinson's disease, 517 patients with sporadic Parkinson's disease, and 559 controls. Three *CHCHD2* mutations in four of 341 index cases from independent families with autosomal dominant Parkinson's disease were detected by *CHCHD2* mutation screening: 182C>T (Thr61Ile), 434G>A (Arg145Gln), and 300+5G>A. Two single nucleotide variants (–9T>G and 5C>T) in *CHCHD2* were confirmed to have different frequencies between sporadic Parkinson's disease and controls, with odds ratios of 2·51 (95% CI 1·48–4·24; p=0·0004) and 4·69 (1·59–13·83, p=0·0025), respectively. One single nucleotide polymorphism (rs816411) was found in *CHCHD2* from a previously reported genome-wide association study; however, there was no significant difference in its frequency between patients with Parkinson's disease and controls in a previously reported genome-wide association study (odds ratio 1·17, 95% CI 0·96–1·19; p=0·22). In SH-SY5Y cells, the 300+5G>A mutation but not the other two mutations caused exon 2 skipping.

Interpretation *CHCHD2* mutations are associated with, and might be a cause of, autosomal dominant Parkinson's disease. Further genetic studies in other populations are needed to confirm the pathogenicity of *CHCHD2* mutations in autosomal dominant Parkinson's disease and susceptibility for sporadic Parkinson's disease, and further functional studies are needed to understand how mutant CHCHD2 might play a part in the pathophysiology of Parkinson's disease.

Funding Japan Society for the Promotion of Science; Japanese Ministry of Education, Culture, Sports, Science and Technology; Japanese Ministry of Health, Labour and Welfare; Takeda Scientific Foundation; Cell Science Research Foundation; and Nakajima Foundation.

Introduction

Parkinson's disease (MIM 168600), which is caused by the death of dopaminergic neurons in the substantia nigra, is the second most common neurodegenerative disorder. Symptoms mainly involve movement, including resting tremor, rigidity, bradykinesia, and postural instability. Most Parkinson's disease cases are sporadic; only about 11% of patients with Parkinson's disease have one or more first-degree relatives diagnosed with Parkinson's disease.[1] Nevertheless, identification of causative genes in rare familial cases can shed new light on the cause of Parkinson's disease. Most monogenic forms of neurodegenerative diseases are autosomal dominant; however, so far, only six genes have been identified for autosomal dominant forms of familial Parkinson's disease.[2–4]

Although the exact mechanisms of dopaminergic cell death are still unclear, discovery of causative genes for Parkinson's disease has enabled several processes to be proposed, such as impairments in protein degradation, oxidative stress, and mitochondrial dysfunction.[5] We aimed to identify a novel causative gene for familial

Parkinson's disease by whole-genome and exome sequencing with next-generation sequencing.

Methods

Study design and participants

Participants were selected from the DNA bank of the Comprehensive Genetic Study on Parkinson's Disease and Related Disorders (CGSPD). The CGSPD bank in the Department of Neurology at Juntendo University School of Medicine (Tokyo, Japan) collects DNA and RNA of patients with typical Parkinson's disease, patients with atypical parkinsonism, and control participants for use in case-control studies, replication studies, and the discovery of novel genetic factors for Parkinson's disease. The CGSPD DNA bank stores samples from over 3500 patients with Parkinson's disease and about 800 controls.

We selected patient and control samples according to the following criteria: participants who had a completed clinical data sheet, participants with no known pathogenic mutations for Parkinson's disease, and participants with no parental consanguinity. Patients who seemed to have an autosomal recessive mode of inheritance were excluded, as were those with a family member with Parkinson's disease but an unknown mode of inheritance. We classified patients who had affected family members in at least two consecutive generations (including the index patient) as having autosomal dominant Parkinson's disease and the remaining patients as having sporadic Parkinson's disease. All patients were diagnosed by neurologists according to the Parkinson's UK Brain Bank clinical diagnostic criteria.[6] Controls, who were hospital staff and volunteers recruited during annual medical check-ups for metabolic syndrome, were confirmed by study neurologists (RS, YK, and SK) to be free of neurological disease. All participants were classed as Japanese according to self-reported racial and ethnic data.

The study was approved by the ethics committee of Juntendo University School of Medicine and all participants gave written informed consent for inclusion in CGSPD, of which this study is a part.

Procedures

For one index patient in our DNA bank, DNA were available for patients with Parkinson's disease and unaffected family members in three generations (family A). Thus, we did linkage analysis and next-generation sequencing to identify a candidate gene in this family. We collected DNA samples from all members of family A who consented to genetic testing (eight affected and five unaffected individuals from family A; figure 1A) and confirmed that they did not have known Parkinson's disease causative gene mutations (appendix). All participants in family A were genotyped using a Genome-Wide human SNP Array 6.0 (Affymetrix, Santa Clara, CA, USA), and we did multipoint parametric linkage analyses with single nucleotide polymorphism (SNP) high throughput linkage analysis system (SNPHitLink)[7] and Merlin software.[8] We selected three patients (A-III-1, A-III-6, and A-III-17) with maximum genetic distance for exome sequencing and one patient (A-II-18) for whole-genome sequencing to complement the regions of difficulty captured by exome sequencing. We did whole-genome sequencing by 100 bp paired-end sequencing on HiSeq2000 (Illumina, San Diego, CA, USA). Sample preparation for exome sequencing was done using the SureSelect Human All Exon Kit (Agilent Technologies, Santa Clara, CA, USA), and samples were subjected to 75 bp paired-end sequencing on a GenomeAnalyzer IIx (Illumina). We did read alignment to the reference human genome (UCSC hg19) with Burrows-Wheeler Aligner version 0.5.9.[9] Single nucleotide variants (SNVs) and indels were detected in each participant by use of SAMtools version 0.1.16.[10] The variants identified by next-generation sequencing were filtered according to the following criteria: location in regions with positive log of odds greater than 1 (appendix); absence from dbSNP132; location in exons or splice sites; being carried in the heterozygous state; prediction to be non-synonymous or cause aberrant splicing; confirmation by Sanger sequencing; and not noted in our unaffected Japanese controls.

We analysed genomic sequences from index cases with autosomal dominant Parkinson's disease, patients with sporadic Parkinson's disease, and control participants by Sanger sequencing with the Applied Biosystems 3130 and 3730 Genetic Analyzer (Life Technologies, Carlsbad, CA, USA) to validate the candidate genes. Primers for Sanger sequencing were designed using ExonPrimer (appendix). The sample size needed for validation was decided on the basis of a previous genetic study that identified a causal gene for neurodegenerative disease and that included 212 controls and data from public databases for the validation of novel variants.[11] We used 1000 Genomes (1089 individuals), dbSNP138, the Human Genetic Variation Database (1208 individuals), and the National Heart, Lung, and Blood Institute (NHLBI) Exome Sequencing Project (ESP) database (6503 individuals) as public databases for the validation.

For cell culture and transfection, cells were seeded onto tissue culture plates for 5 days (SK-N-SH and SH-SY5Y cells) or 24 h (HeLa cells) before transfection. SH-SY5Y cells were used for splicing assays, SK-N-SH cells were used for localisation assays, and HeLa cells were used for splicing, localisation, and immunoelectron microscopy analyses. Cultured cells were transfected using Lipofectamine 2000 reagent (Life Technologies), according to the manufacturer's recommendations.

For splicing analysis, we cloned wild-type and mutant genomic *CHCHD2* DNA fragments (182C>T, 300+5G>A, and 434G>A) into pCR-Blunt II-TOPO vector (Life Technologies) and then transferred them to *KpnI-XhoI* sites in pcDNA3.1/myc-His-A (Life Technologies), generating pcDNA3.1-CHCHD2 (wild-type, 182C>T, 300+5G>A, and 434G>A). *CHCHD2* exon 2 (wild-type

(H Saiki MD); **Division of Neurology and Molecular Brain Science, Kobe University Graduate School of Medicine, Kobe, Japan** (W Satake MD, Prof T Toda MD); **Department of Neurology, Mie University Graduate School of Medicine** (R Sasaki MD) **and Kii ALS/PDC Research Center, Mie University Graduate School of Regional Innovation Studies** (Prof Y Kokubo MD), **Tsu, Japan; and Department of Neurology and Medicine, School of Nursing, Suzuka University of Medical Science, Suzuka, Japan** (Prof S Kuzuhara MD)

Correspondence to:
Prof Nobutaka Hattori, Department of Neurology, Juntendo University School of Medicine, 2-1-1 Hongo, Bunkyo-ku, Tokyo 113-8421, Japan
nhattori@juntendo.ac.jp

For **ExonPrimer** see http://ihg.gsf.de/ihg/ExonPrimer.html

See Online for appendix

and 300+5G>A) with flanking intronic sequence (52 nucleotides upstream and 14 nucleotides downstream) was subcloned into pSPL3,[12] generating pSPL3-CHCHD2 (to analyse abberant exon 2 splicing of 300+5G>A). Total RNA was extracted 24 h after transfection using TRI Reagent (Life Technologies) followed by RQ1 DNase (Promega, Madison, WI, USA) treatment. cDNA was synthesised with random primers using Superscript II reverse transcriptase (Life Technologies) or ReverTra Ace (TOYOBO, Osaka, Japan). Two primer pairs were used for amplification to detect mutation-induced exon skipping of the transfected pcDNA splicing minigene (appendix). α-^{32}P-uridine triphosphate-labelled RNA was synthesised in the 5′ splice site of *CHCHD2* exon 2 using the Riboprobe in-vitro transcription system (Promega) with a PCR-amplified fragment, according to the manufacturer's instructions. We did an RNA-electrophoretic mobility

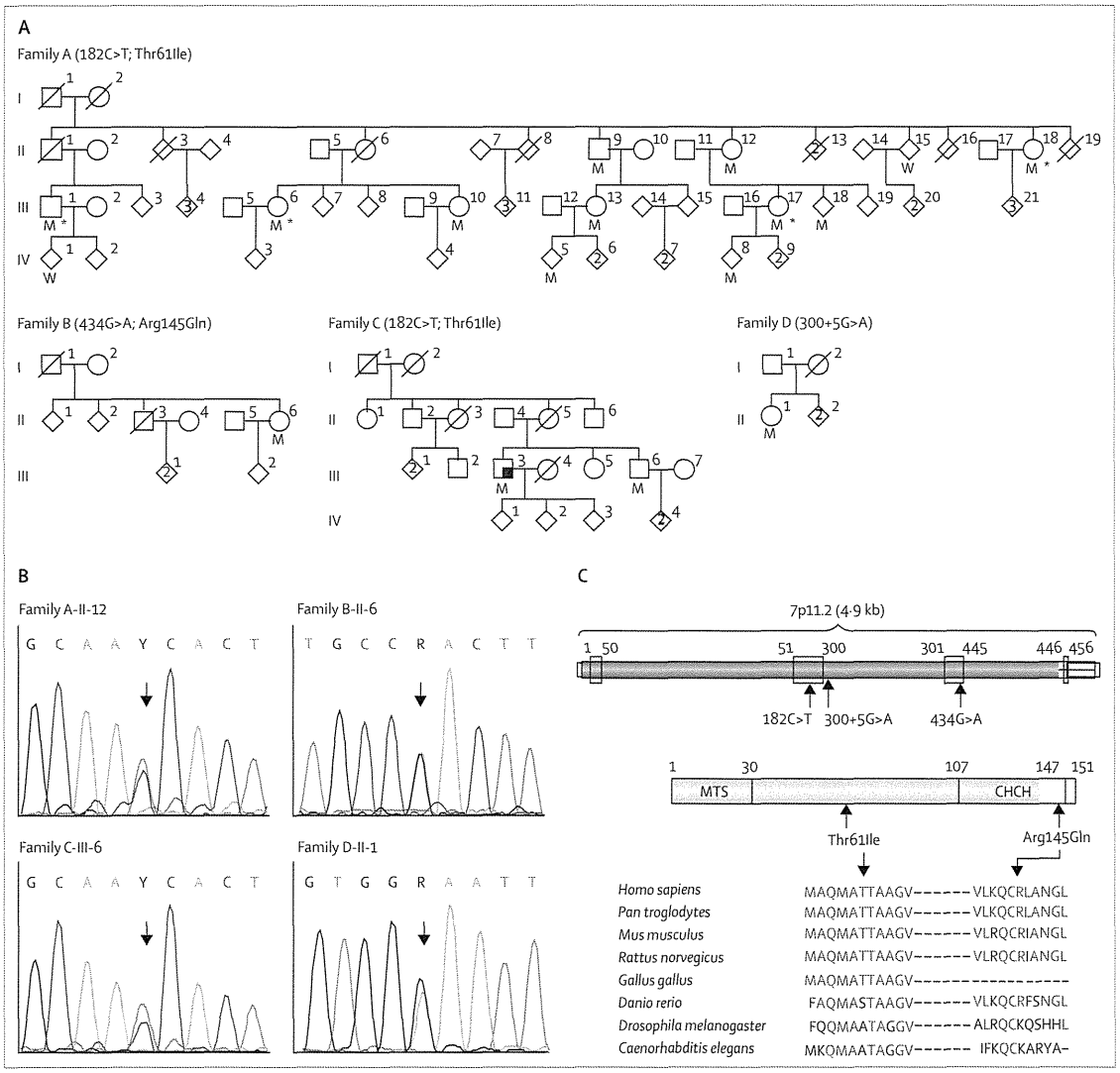

***Figure 1:* *CHCHD2* mutations in four Japanese families with autosomal dominant Parkinson's disease**
(A) Pedigrees of families with *CHCHD2* mutations. M=heterozygous *CHCHD2* mutation. W=wild-type. Blue symbols represent affected individuals. Red symbols represent unaffected individuals. Numbers within red symbols represent number of unaffected offspring. The quarter-filled symbol represents an individual with essential tremor. Squares represent men. Circles represent women. Diamonds represent sex masked to protect privacy of unaffected individuals. Lines through symbols represent deceased individuals. *Participants analysed by next-generation sequencing. (B) Sequence electropherograms of identified *CHCHD2* mutations. Arrows=mutated bases. (C) Schematic representation of the *CHCHD2* locus and CHCHD2 structure. Genomic locations of identified *CHCHD2* mutations are shown in the upper part of the panel. Boxes on the line represent exons. Aminoacid locations of mutations and sequence alignment with various species are shown in the lower part. NCBI RefSeq accession numbers are as follows: *Homo sapiens*, NP_057223.1; *Pan troglodytes*, XP_003318501.1; *Mus musculus*, NP_077128.2; *Rattus norvegicus*, NP_001015019.1; *Gallus gallus*, NP_001006218.1; *Danio rerio*, NP_957061.1; *Drosophila melanogaster*, NP_573196.1; and *Caenorhabditis elegans*, NP_497826.1. CHCH=coiled-coil-helix-coiled-coil-helix domain. MTS=mitochondrial targeting sequence.

shift assay as described by Ohe and colleagues.[13] The appendix provides probe information, details of antibodies used, and supplemental methods.

Statistical analysis

SNPs with a Hardy–Weinberg equilibrium p value greater than 0·05, a minimum call rate of 1 in controls, a maximum confidence greater than 0·02, a minimum interval of 100 kb, and a minimum minor allele frequency of 0·2 were selected using SNPHitLink. We did parametric multipoint linkage analysis using Merlin software, with a disease frequency of 0·0001. The phenotypes of unaffected siblings and children of patients were described as 0 (missing phenotypes). We did case-control studies using the genotype data of ten variants that were detected in sporadic Parkinson's disease or controls, or both. We used the Fisher's exact test to calculate the significance of allele frequencies between patients with sporadic Parkinson's disease and unaffected controls. We calculated odds ratios (ORs) and 95% CIs of minor alleles found in this study using JMP 8 (SAS Institute, Drive Cary, NC, USA). In association analyses, we used the Bonferroni correction to adjust for multiple testing (ten tests), after which p values of 0·005 or lower were regarded as statistically significant, as detailed in a previous study.[14]

Role of the funding source

The funders of the study had no role in study design, data collection, data analysis, data interpretation, or writing of the report. MF and NH had full access to all the data in the study and had final responsibility for the decision to submit for publication. The other authors had access to all data except for the sequence data acquired from next-generation sequencing, to protect the privacy of personal data.

Results

The mean age at onset of the participating patients in family A (eight patients) was 55·5 years (SD 4·8; range 48–61). For validation and case-control analysis, we obtained DNA samples from 340 additional index patients with autosomal dominant Parkinson's disease, 517 patients with sporadic Parkinson's disease, and 559 controls (16 hospital staff and 543 volunteers recruited during medical check-ups; table 1).

Using next-generation sequencing, we detected a cumulative total of over 2·3 million variants in the four patients who were assessed (table 2; appendix). Our filtering criteria were satisfied by only one variant (table 2; appendix). The heterozygous 182C>T (Thr61Ile) mutation in coiled-coil-helix–coiled-coil-helix domain containing 2 (*CHCHD2*; RefSeq accession number NM_016139.2) cosegregated with Parkinson's disease in family A as assessed by Sanger sequencing of eight affected and five unaffected individuals (figure 1A and B). *CHCHD2* is located on chromosome 7p11.2 and contains four exons that encode 151 aminoacids with a predicted N-terminal mitochondrial targeting sequence (figure 1C). To validate the results of the initial genome-wide linkage analysis of family A (appendix), we did parametric multipoint linkage analysis using six microsatellites mapped to the 5′ and 3′flanking regions of *CHCHD2*. Parametric multipoint linkage analysis by Merlin yielded a maximum log of odds score of 3·009 at D7S506 (appendix). Additionally, we did two-point linkage analysis using the 182C>T mutation as a genetic marker with a frequency of 0·0018 (1 in 560; 559 controls were sequenced in this study). As a result, the maximum log of odds score was 3·004.

To confirm whether *CHCHD2* is associated with autosomal dominant Parkinson's disease, we screened 340 index cases with autosomal dominant Parkinson's disease by Sanger sequencing and detected three additional patients with *CHCHD2* variants (families B–D; figure 1A and B). None of the three variants were noted in the 559 unaffected Japanese controls (table 3). None of the three variants detected in this study were found in 1000 Genomes, the Human Genetic Variation Database (table 3), the NHLBI ESP, or dbSNP138 (data not shown). Although the Thr61Ile variant was identified in patients from families A and C, independent founders were estimated by haplotype analysis (appendix). Altogether, we identified two missense mutations (182C>T, Thr61Ile, and 434G>A, Arg145Gln) and one splice-site mutation (300+5G>A) from four independent families with autosomal dominant Parkinson's disease.

	Number of participants	Age at onset (years)	Age at sampling (years)	Women:men ratio
Autosomal dominant Parkinson's disease	340	51·42 (13·81, 8–83)	57·99 (13·29, 17–85)	1·27
Sporadic Parkinson's disease	517	48·94 (15·11, 5–88)	57·38 (14·53, 12–92)	1·06
Controls	559	NA	58·74 (11·72, 28–89)	1·57

Data are mean (SD, range) unless otherwise specified. 340 patients were from different, independent, families, whereas family A included eight affected and five unaffected individuals; thus, family A is not included here. NA=not applicable.

Table 1: **Characteristics of participants for additional mutation screening**

	Number of variants
Total variants	2 312 760
In the linkage region	200 075
Not in db132	38 969
In exon or splice site	1018
Heterozygous	304
Predicted to be damaging*	10
Validated by Sanger sequencing	1
Not in 559 controls	1

*Predicted to be non-synonymous or cause aberrant splicing.

Table 2: **Variant filtering**

	Variant		rs number	Alternative minor allele frequency					Sporadic PD vs controls	
	cDNA	Aminoacid		Autosomal dominant PD (n=340)	Sporadic PD (n=517)	Controls (n=559)	1000 Genomes	HGVD[15]	OR (95% CI)*	p value†
chr7:56174117	-11G>A	5'UTR	rs200226056	0·000	0·000	0·00099	0·0014	ND	..	..
chr7:56174115	-9T>G	5'UTR	rs10043	0·041	0·048	0·020	0·13	0·044	2·51 (1·48–4·24)	0·0004
chr7:56174102	5C>T	Pro2Leu	rs142444896	0·035	0·018	0·004	0·008	0·013	4·69 (1·59–13·83)	0·0025
chr7:56172172	51-4A>G	Splice site	Unknown	0.000	0·00097	0·005	ND	0·004	0·19 (0·02–1·66)	0·1189
chr7:56172171	51-3C>T‡	Splice site	rs201791644	0·002	0·00097	0·000	0·00046	0·003	..	..
chr7:56172037	182C>T	Thr61Ile	Novel	0·006	0·000	0·000	ND	ND	..	..
chr7:56171964	255T>A	Ser85Arg	rs182992574	0·002	0·000	0·000	0·00092	0·002	..	..
chr7:56171914	300+5G>A	Splice site	Novel	0·002	0·000	0·000	ND	ND	..	..
chr7:56170571	434G>A	Arg145Gln	Novel	0·002	0·000	0·000	ND	ND	..	..
chr7:56169419	*125G>A	3'UTR	rs8406	0·041	0·048	0·027	0·13	ND	1·85 (1·16–2·94)	0·0112

..=not calculated because the genotypes of all of the patients with sporadic PD or controls were the major allele. HGVD=Human Genetic Variation Database.[15] ND=no data were found in database. OR=odds ratio. PD=Parkinson's disease. UTR=untranslated region. *Calculated for the minor allele. †Fisher's exact test. ‡Did not cosegregate in an autosomal dominant PD family.

Table 3: **Alternative minor allele frequencies of identified *CHCHD2* variants**

Thr61 and Arg145 are conserved residues among vertebrates (figure 1C), suggesting these sites may be of functional importance. The substitutions Thr61Ile and Arg145Gln are predicted to be pathogenic or disease causing by Polyphen2,[16] MutationTaster,[17] and SIFT.[18] Furthermore, we analysed the 300+5G>A mutation using Human Splicing Finder (version 2.4.1)[19] to predict whether it affects *CHCHD2* splicing. The 300+5G>A mutation at the 5′ splice site decreased the Human Splicing Finder score from 88·2 to 76·0, and the MaxEnt score from 6·71 to 1·62. The SD-score[20] similarly predicted that 300+5G>A causes aberrant splicing and is likely to be a splicing mutation.

To assess whether any of the mutations affect splicing in the human SH-SY5Y neuroblastoma cell line, we cloned wild-type and mutant full-length (4921 bp) genomic DNA fragments into the pcDNA3.1 mammalian expression vector. As shown in figure 2A, exon 2 splicing was not affected by pcDNA-*CHCHD2* wild-type, 182C>T, or 434G>A, but the 300+5G>A mutation caused exon 2 skipping. None of the clones affected exon 3 splicing (appendix).

We further analysed the 300+5G>A mutation in HeLa cells by inserting *CHCHD2* exon 2 and flanking introns between the two proprietary constitutive exons of a modified exon-trapping vector, pSPL3. In this heterologous context, the 300+5G>A mutation caused *CHCHD2* exon 2 exclusion (figure 2B). The exon 2-excluded mRNA generated a premature termination codon 24 nucleotides upstream of the last exon junction, and thus should be resistant to non-sense-mediated mRNA decay. The band with intermediate mobility between the exon-containing and exon-skipped bands was sequenced and shown to result from activation of an upstream cryptic-5′ splice site at position 161 in *CHCHD2* exon 2. This mRNA was predicted to be subject to non-sense-mediated mRNA decay due to a premature termination codon generated 98 nucleotides upstream of the last exon junction. We tested U1 small nuclear ribonucleoprotein (snRNP) binding to wild-type and 300+5G>A mutant 5′ splice sites with RNA electrophoresis mobility shift assays. We noted decreased U1 snRNP-binding in HeLa nuclear extracts for 300+5G>A compared with wild-type 5′ splice site RNA (figure 2C, lanes 4 and 8). We verified the mobility of the complex using purified U1 snRNP.[13] Database searches for a truncating mutation in *CHCHD2* detected a non-sense SNV, Tyr99Stop, in 1000 Genomes and dbSNP138 databases, with an allelic frequency of one in 2178. No other protein-truncating mutations were registered in the Human Genetic Variation Database or the NHLBI ESP database. This is a rare non-sense SNV and we are unable to say whether it is related to pathogenicity in Parkinson's disease or other diseases.

To investigate whether *CHCHD2* might be a susceptibility gene for sporadic Parkinson's disease, we sequenced all *CHCHD2* exons, including splice junctions, in 517 patients with sporadic Parkinson's disease and 559 controls. Two SNVs had significantly different frequencies (–9T>G, OR 2·51, 95% CI 1·48–4·24, p=0·0004; and 5C>T, 4·69, 1·59–13·83, p=0·0025; table 3). The frequencies of several variants in the control participants were slightly different to those in public databases (table 3). To confirm the link between *CHCHD2* variants and risk of sporadic Parkinson's disease, we examined a previously reported genome-wide association study on sporadic Parkinson's disease in Japanese people.[21] Although one SNP (rs816411) was found on the intron of *CHCHD2*, there was no significant difference in its frequency between patients and control participants in this genome-wide association study (OR 1·17, 95% CI 0·96–1·19, p=0·22, Cochran-Armitage trend test).[21]

CHCHD2 has a predicted N-terminal mitochondrial targeting sequence according to the UniProt database; therefore, we investigated whether CHCHD2 is located in mitochondria. Western blot analysis of subcellular fractions revealed that endogenous CHCHD2 is present in mitochondria (appendix). Furthermore, findings from confocal microscopy studies showed that exogenously expressed CHCHD2 localises to mitochondria, whereas CHCHD2 that has had the mitochondrial targeting sequence deleted does not (appendix). Immunoelectron microscopy and trypsin digestion assays showed that CHCHD2 is mainly localised in the intermembrane space (appendix). No localisation differences were noted between wild-type and missense mutants (appendix).

Table 4 summarises the clinical features of the patients with *CHCHD2* mutations. The mean age at onset of Parkinson's disease was 56·2 years (SD 8·1, range 40–67). Although a patient from family C (C-III-3; figure 1), who was examined and from whom DNA was collected after additional mutation screening with 340 index cases, mainly showed only upper limb tremor-like essential tremor, other patients presented with typical parkinsonian features, including bradykinesia, rigidity, and gait disturbance, with symptoms responsive to levodopa that are consistent with the UK Brain Bank Parkinson's disease criteria.[6] Additionally, we detected three asymptomatic carriers with heterozygous 182C>T (Thr61Ile) mutations (A-III-18, A-IV-5, and A-IV-8). Their ages at sampling were 55 years, 56 years, and 35 years, respectively.

Discussion

In this study, we show that the heterozygous 182C>T (Thr61Ile) mutation in *CHCHD2* cosegregated with Parkinson's disease in a Japanese family with autosomal dominant Parkinson's disease. We identified three *CHCHD2* variants, none of which was present in controls, and our findings suggest that *CHCHD2* is a novel gene for autosomal dominant Parkinson's disease (panel).

CHCHD2 belongs to the CHCHD protein family, which are small proteins (about <18 kDa) containing twin cysteine-x9-cysteine motifs. CHCHD proteins localise to the mitochondrial intermembrane space via the Mia40 and Erv1 disulphide relay system.[24] Proteins with the cysteine-x9-cysteine motif are involved in biogenesis and regulation of enzymes in the mitochondrial respiratory chain, from yeast to mammals.[24] In particular, CHCHD2 seems to be closely linked to cytochrome c oxidase (COX), because COX2 protein concentrations and COX activity are affected by *CHCHD2* knock down.[22,23] Moreover, CHCHD2 acts as an antiapoptotic factor in cancer cells.[25] Although further functional studies are needed to investigate how mutant CHCHD2 plays a part in Parkinson's disease in mitochondria, the combination of previously reported CHCHD2 functions and our findings suggest that mitochondrial respiration is the link to Parkinson's disease.

We identified *CHCHD2* mutations not only in patients with Parkinson's disease, but also in a patient with essential tremor from the same family. Although we do not have any dopamine transporter scan data to check for any evidence of a dopaminergic deficit, an association

For the **UniProt database** see http://www.uniprot.org

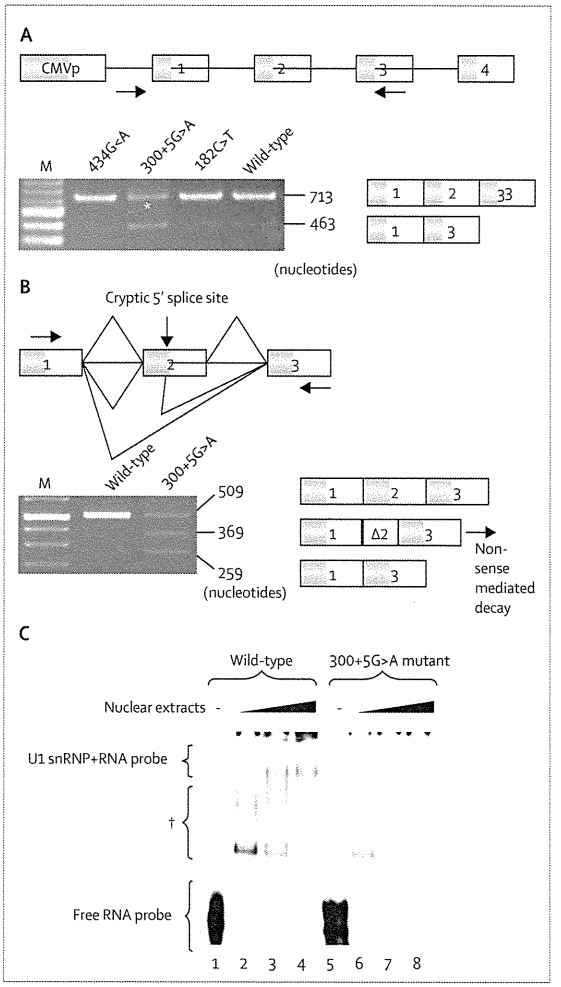

Figure 2: **Splicing assay of *CHCHD2* 300+5G>A**
(A) pcDNA-*CHCHD2*- 300+5G>A induced exon 2 skipping in SH-SY5Y cells, whereas 434G>A, 182C>T, or wild-type did not. *A faint band with intermediate mobility was present between exon 2-containing and exon 2-excluded bands. (B) pSPL3-*CHCHD2*-exon 2- 300+5G>A generated an exon 2-skipped transcript and a transcript with partial exon 2-inclusion via activation of an upstream cryptic 5′ splice site (arrow above exon 2). The arrows next to exons 1 and 3 show the position of primers used in the analyses. Triangles above the gene schematic denote normal splicing between exons 1 and 2, and 2 and 3, which results in a transcript with all three exons shown as a transcript bar below; the two triangles immediately below the line refer to the middle transcript bar with partial exon 2, and the lowest triangle refers to the lowest transcript bar with completely skipped exon 2. Numbers on the right side of the electrophoresis bands show their size. (C) Binding of *CHCHD2* exon 2-wild-type and 300+5G>A-mutant 5′ splice sites to U1 snRNP was measured using increasing amounts of HeLa nuclear extracts (3 μg, 6 μg, and 12 μg). Binding of the 5′ splice site probe to U1 snRNP was compromised with HeLa nuclear extracts. CMVp=cytomegalovirus promoter. M=100 bp DNA marker. snRNP=small nuclear ribonucleoprotein. †Bandshift of incomplete U1snRNP complexes.

	A-II-9	A-II-12	A-II-18	A-III-1	A-III-6	A-III-10	A-III-13	A-III-17	B-II-6	C-III-3	C-III-6	D-II-1
Sex	M	W	W	M	W	W	W	W	W	M	M	W
Age at onset (years)	60	61	55	57	59	49	55	48	67	10	40	67
Age at examination (years)	83	81	69	67	63	50	57	58	72	50	43	68
Disease duration (years)	23	20	14	10	4	1	2	10	5	40	3	1
Initial symptoms	Resting tremor	Bradykinesia	Bradykinesia	Bradykinesia	Resting tremor	Resting tremor	Bradykinesia	Resting tremor	Resting tremor	Fine tremor	Resting tremor	Gait disturbance
Hoehn and Yahr stage (on/off)	5/5	4/ND	ND/ND	3/ND	3/3	2/ND	2/ND	3/ND	3/4	ND/ND	2/ND	ND/3
Resting tremor	+	+	+	+	+	+	–	+	+	+ (fine tremor)	+	–
Bradykinesia	+	+	+	+	+	+	+	+	–	–	+	+
Rigidity	+	+	+	+	+	+	+	+	–	–	+	+
Postural instability	–	–	+	+	+	–	+	+	–	–	–	+
Asymmetry at onset	+	–	+	+	+	+	+	–	+	–	+	+
Clinical response to levodopa	+	ND	+	+	+	ND	+	+	+	ND	+	ND
Wearing off	–	ND	+	–	+	ND	–	+	–	ND	–	ND
On/off phenomenon	–	ND	–	–	–	ND	–	–	+	ND	–	ND
Levodopa-induced dyskinesia	–	ND	+	–	+	ND	–	–	–	ND	–	ND
Hyper-reflexia	–	–	–	–	+	+	–	–	+	–	–	+
Orthostatic hypotension	–	–	–	–	+	–	+	–	–	–	–	–
Constipation	–	+	+	+	+	–	+	–	–	–	–	+
Depression	–	–	–	–	–	–	–	–	–	–	–	+
Smell disturbance	–	–	–	–	–	–	–	–	–	–	–	+

All patients also had gait disturbance. No patients had urinary urgency, hallucinations, delusion, dementia, mental retardation, rapid eye movement sleep behaviour disorder, or restless legs syndrome. M=man. ND=not done. W=woman. –=not present. +=present.

Table 4: **Clinical characteristics of patients with *CHCHD2* mutations**

Panel: Research in context

Systematic review

We searched PubMed, in English, until Dec 11, 2014, for known genes for autosomal dominant Parkinson's disease using the terms "SNCA", "LRRK2", "VPS35", "EIF4G1", "DCTN1" and "DNAJC13". We also searched PubMed for studies published in English using the search terms "CHCHD2", "CHCHD", "Gene AND Parkinson's disease", "import AND assembly of IMS", and "Mic17" until Dec 11, 2014.

Interpretation

We show that (1) all affected individuals in family A who had genetic tests harboured a mutation in *CHCHD2*; (2) the log of odds score was greater than 3; (3) the detected mutations were not found in our control cohort or public variant databases; (4) different mutations in the same gene were found among four families with the same disease; and (5) all detected mutations were predicted to be pathogenic by a mutations algorithm. Although this is strong evidence that *CHCHD2* mutations are associated with Parkinson's disease, only one mutation (182C>T, Thr61Ile) was confirmed to cosegregate with autosomal dominant Parkinson's disease in this study. CHCHD2 has been implicated in mitochondrial respiration and is involved in cytochrome C oxidase activity,[22,23] but no previous reports had shown that *CHCHD2* mutations are associated with disease.

between essential tremor and Parkinson's disease has been suggested by many clinical, epidemiological, neuroimaging, and genetic studies.[26] Additionally, a large family from Arkansas, USA, with Parkinson's disease, essential tremor, and restless legs syndrome has been reported.[27] *CHCHD2* mutations might be identified in this family, but to our knowledge the family has not been tested for *CHCHD2* mutations. We could not make any conclusions regarding the relation between essential tremor and *CHCHD2* mutations because only one patient with essential tremor and a *CHCHD2* mutation was detected in this study. Further studies are needed to identify whether *CHCHD2* is involved in both Parkinson's disease and essential tremor, or whether essential tremor happens to coincide with Parkinson's disease in the same family because of reduced penetrance. Recent studies have reported that *CHCHD2* expression is increased in neural stem cell lines derived from a patient with Huntington's disease (MIM 143100) and in HEK-293 cells under hypoxic conditions (4% oxygen).[22,28,29] Based on these observations, *CHCHD2* might be involved in various neurodegenerative diseases and cerebral infarction (MIM 601367).

Causative genes for mendelian forms of Parkinson's disease play an important part in mitochondrial clearance, and the clearance of damaged mitochondria is a key mechanism in the pathogenesis of Parkinson's disease and needs to be better understood. *PARK2* (MIM 602544) and *PINK1* (MIM 608309) are well known causative genes for early-onset autosomal recessive Parkinson's disease. Findings from functional studies have revealed that Parkin E3 ubiquitin ligase is fully activated by PINK1-dependent phosphorylation of both Parkin and ubiquitin on damaged mitochondria in the first phase of PINK1/parkin-mediated mitophagy.[30,31] MIX17 (YMR002W), the

yeast homolog of CHCHD2, is regulated by the ubiquitin-proteasome system.[32] Although there has been no evidence of a relation between CHCHD2 and mitophagy, whether CHCHD2 is involved in PINK1/parkin-mediated mitophagy should be investigated.

Although the Thr61Ile mutation of *CHCHD2* was confirmed in independent probands and cosegregates with Parkinson's disease, the Arg145Gln and splicing (300+5G>A) mutations were found in only one patient in a small family with autosomal dominant Parkinson's disease. Whether or not these two mutations are linked to Parkinson's disease remains unclear. We would have liked to confirm these findings by undertaking mutation screening of patients and unaffected members of families B and D, but unfortunately the patients in this study declined access to other family members. Furthermore, we could not collect RNA samples from patients with 300+5G>A mutations, which produced the splicing abnormality in SH-SY5Y cells.

Our findings differ from those from a previously reported genome-wide association study.[21] We are unsure whether our case-control study detected false positive results because of the small sample size or whether the genome-wide association study could not detect positive variants for Parkinson's disease risk because of the low allele frequencies of SNVs mapped on the *CHCHD2* region.

Contributors

MF, YM, KOhn, and NH were responsible for the concept and design of the study. MF, SS, and KOhe wrote the first draft of the paper. MF, KOhe, TA, NF, JY, SS, HY, WS, KM, KOhn, and NH revised the manuscript. MF, KOhe, TA, NF, JY, SS, YL, KOg, MA, HY, HT, KN, KH, HS, WS, KM, TT, YM, YU, KOhn, and NH acquired, analysed, and interpreted data. RS, YK, and SK collected and characterised control samples. All authors read and commented on drafts of the manuscript before submission.

Declaration of interests

MF and NH have a patent pending relating to this work. YM has received personal fees from FP Pharmaceutical, Otsuka Pharmaceutical, Abbvie, and Kyowa Hakko-Kirin. NH has received personal fees from Hisamitsu Pharmaceutical, Otsuka Pharmaceutical, Novartis Pharma, GlaxoSmithKline, Nippon Boehringer Ingelheim, FP Pharmaceutical, Dai-Nippon Sumitomo Pharma, Eisai, Kissei Pharmaceutical, Janssen Pharmaceutical, Nihon Medi-physics, Astellas Pharma, and Kyowa Hakko-Kirin. All other authors declare no competing interests.

Acknowledgments

We thank Yoko Imamichi for her assistance. We received a Grant-in-Aid for Scientific Research on Innovative Areas (25129707 to MF, 25111007 to SS, 25110720 to WS, 22129006 to TT, 23111004 to YU, 25118508 to KOhn, and 23111003 to NH), and a Grant-in-Aid for the Program for the Strategic Research Foundation at Private Universities from the Japanese Ministry of Education, Culture, Sports, Science and Technology; a Grant-in-Aid for Young Scientists (24790903 to TA, 25860725 to YL, 23689046 to SS, 25860726 to KN, 25713015 to WS, and, 26870175 to KM); a Grant-in-Aid for Challenging Exploratory Research (24659435 to SS, 25670420 to WS, 25670099 to YU and 25670164 to KOhn); a Grant-in-Aid for Scientific Research from the Japan Society for the Promotion of Science (25461291 to MF, 24591920 to KOhe, 24500868 to NF, 25305030 to YK, 24390221 to KOhn, and 24390224 to NH); a Grant-in-Aid for Health Labour Sciences Research Grant (H24-Nanchitou-Nan-Ippan-058 to YK, H26-Nanchitou-Nan-Ippan-085 to YK, TT, and NH; H23-Jitsuyouka-Nanbyou-Ippan-015 to TT; H26-Itaku-Nan-Ippan-037 to TT and NH; and H26-Itaku-Nan-Ippan-024 to KOhn) from the Japanese Ministry of Health, Labour and Welfare; and grants from the Life Science Foundation, the Takeda Scientific Foundation, the Cell Science Research Foundation, and the Nakajima Foundation (SS).

References

1 Shino MY, McGuire V, Van Den Eeden SK, et al. Familial aggregation of Parkinson's disease in a multiethnic community-based case-control study. *Mov Disord* 2010; **25:** 2587–94.
2 Singleton AB, Farrer MJ, Bonifati V. The genetics of Parkinson's disease: progress and therapeutic implications. *Mov Disord* 2013; **28:** 14–23.
3 Lautier C, Goldwurm S, Dürr A, et al. Mutations in the GIGYF2 (TNRC15) gene at the PARK11 locus in familial Parkinson disease. *Am J Hum Genet* 2008; **82:** 822–33.
4 Vilariño-Güell C, Rajput A, Milnerwood AJ, et al. DNAJC13 mutations in Parkinson disease. *Hum Mol Genet* 2014; **23:** 1794–801.
5 Schapira AH, Olanow CW, Greenamyre JT, Bezard E. Slowing of neurodegeneration in Parkinson's disease and Huntington's disease: future therapeutic perspectives. *Lancet* 2014; **384:** 545–55.
6 Hughes AJ, Daniel SE, Kilford L, Lees AJ. Accuracy of clinical diagnosis of idiopathic Parkinson's disease: a clinico-pathological study of 100 cases. *J Neurol Neurosurg Psychiatry* 1992; **55:** 181–84.
7 Fukuda Y, Nakahara Y, Date H, et al. SNP HiTLink: a high-throughput linkage analysis system employing dense SNP data. *BMC Bioinformatics* 2009; **10:** 121.
8 Abecasis GR, Cherny SS, Cookson WO, Cardon LR. Merlin—rapid analysis of dense genetic maps using sparse gene flow trees. *Nat Genet* 2002; **30:** 97–101.
9 Li H, Durbin R. Fast and accurate short read alignment with Burrows-Wheeler transform. *Bioinformatics* 2009; **25:** 1754–60.
10 Li H, Handsaker B, Wysoker A, et al. The Sequence Alignment/Map format and SAMtools. *Bioinformatics* 2009; **25:** 2078–79.
11 Saitsu H, Nishimura T, Muramatsu K, et al. De novo mutations in the autophagy gene *WDR45* cause static encephalopathy of childhood with neurodegeneration in adulthood. *Nat Genet* 2013; **45:** 445–49.
12 Masuda A, Shen XM, Ito M, Matsuura T, Engel AG, Ohno K. hnRNP H enhances skipping of a nonfunctional exon P3A in CHRNA1 and a mutation disrupting its binding causes congenital myasthenic syndrome. *Hum Mol Genet* 2008; **17:** 4022–35.
13 Ohe K, Mayeda A. HMGA1a trapping of U1 snRNP at an authentic 5′ splice site induces aberrant exon skipping in sporadic Alzheimer's disease. *Mol Cell Biol* 2010; **30:** 2220–28.
14 Sham PC, Purcell SM. Statistical power and significance testing in large-scale genetic studies. *Nat Rev Genet* 2014; **15:** 335–46.
15 Narahara M, Higasa K, Nakamura S, et al. Large-scale east-Asian eQTL mapping reveals novel candidate genes for LD mapping and the genomic landscape of transcriptional effects of sequence variants. *PLoS One* 2014; **9:** e100924.
16 Adzhubei IA, Schmidt S, Peshkin L, et al. A method and server for predicting damaging missense mutations. *Nat Methods* 2010; **7:** 248–49.
17 Schwarz JM, Rödelsperger C, Schuelke M, Seelow D. MutationTaster evaluates disease-causing potential of sequence alterations. *Nat Methods* 2010; **7:** 575–76.
18 Kumar P, Henikoff S, Ng PC. Predicting the effects of coding non-synonymous variants on protein function using the SIFT algorithm. *Nat Protoc* 2009; **4:** 1073–81.
19 Desmet, FO, Hamroun D, Lalande M, Collod-Beroud G, Claustres M, Beroud C. Human Splicing Finder: an online bioinformatics tool to predict splicing signals. *Nucleic Acid Res* 2009; **37:** e67.
20 Sahashi K, Masuda A, Matsuura T, et al. In vitro and in silico analysis reveals an efficient algorithm to predict the splicing consequences of mutations at the 5′ splice sites. *Nucleic Acids Res* 2007; **35:** 5995–6003.
21 Satake W, Nakabayashi Y, Mizuta I, et al. Genome-wide association study identifies common variants at four loci as genetic risk factors for Parkinson's disease. *Nat Genet* 2009; **41:** 1303–07.
22 Aras S, Bai M, Lee I, Springett R, Hüttemann M, Grossman LI. MNRR1 (formerly CHCHD2) is a bi-organellar regulator of mitochondrial metabolism. *Mitochondrion* 2015 **20:** 43–51.

23 Baughman JM, Nilsson R, Gohil VM, Arlow DH, Gauhar Z, Mootha VK. A computational screen for regulators of oxidative phosphorylation implicates SLIRP in mitochondrial RNA homeostasis. *PLoS Genet* 2009; **5:** e1000590.

24 Longen S, Bien M, Bihlmaier K, et al. Systematic analysis of the twin cx(9)c protein family. *J Mol Biol* 2009; **393:** 356–68.

25 Liu Y, Clegg HV, Leslie PL, et al. CHCHD2 inhibits apoptosis by interacting with Bcl-x L to regulate Bax activation. *Cell Death Differ* 2014; published online Dec 5. DOI:10.1038/cdd.2014.194.

26 Fekete R, Jankovic J. Revisiting the relationship between essential tremor and Parkinson's disease. *Mov Disord* 2011; **26:** 391–98.

27 Puschmann A, Pfeiffer RF, Stoessl AJ, et al. A family with parkinsonism, essential tremor, restless legs syndrome, and depression. *Neurology* 2011; **76:** 1623–30.

28 Feyeux M, Bourgois-Rocha F, Redfern A, et al. Early transcriptional changes linked to naturally occurring Huntington's disease mutations in neural derivatives of human embryonic stem cells. *Hum Mol Genet* 2012; **21:** 3883–95.

29 Aras S, Pak O, Sommer N, et al. Oxygen-dependent expression of cytochrome c oxidase subunit 4-2 gene expression is mediated by transcription factors RBPJ, CXXC5 and CHCHD2. *Nucleic Acids Res* 2013; **41:** 2255–66.

30 Kondapalli C, Kazlauskaite A, Zhang N, et al. PINK1 is activated by mitochondrial membrane potential depolarization and stimulates Parkin E3 ligase activity by phosphorylating Serine 65. *Open Biol* 2012; **2:** 120080.

31 Koyano F, Okatsu K, Kosako H, et al. Ubiquitin is phosphorylated by PINK1 to activate parkin. *Nature* 2014; **510:** 162–66.

32 Bragoszewski P, Gornicka A, Sztolsztener ME, Chacinska A. The ubiquitin-proteasome system regulates mitochondrial intermembrane space proteins. *Mol Cell Biol* 2013; **33:** 2136–48.

Neurobiology of Disease

The Role of Pak-Interacting Exchange Factor-β Phosphorylation at Serines 340 and 583 by PKCγ in Dopamine Release

Toshihiko Shirafuji,[1] Takehiko Ueyama,[1] Ken-ichi Yoshino,[1] Hideyuki Takahashi,[1] Naoko Adachi,[1] Yukio Ago,[2] Ken Koda,[2] Tetsuaki Nashida,[2] Naoki Hiramatsu,[2] Toshio Matsuda,[2] Tatsushi Toda,[3] Norio Sakai,[4] and Naoaki Saito[1]

[1]Laboratory of Molecular Pharmacology, Biosignal Research Center, Kobe University, Kobe 657-8501, Japan, [2]Laboratory of Medicinal Pharmacology, Graduate School of Pharmaceutical Sciences, Osaka University, Suita, Osaka 565-0871, Japan, [3]Division of Neurology/Molecular Brain Science, Kobe University Graduate School of Medicine, Kobe 650-0017, Japan, and [4]Department of Molecular and Pharmacological Neuroscience, Graduate School of Biomedical Sciences, Hiroshima University, Hiroshima 734-8551, Japan

Protein kinase C (PKC) has been implicated in the control of neurotransmitter release. The AS/AGU rat, which has a nonsense mutation in PKCγ, shows symptoms of parkinsonian syndrome, including dopamine release impairments in the striatum. Here, we found that the AS/AGU rat is PKCγ-knock-out (KO) and that PKCγ-KO mice showed parkinsonian syndrome. However, the PKCγ substrates responsible for the regulated exocytosis of dopamine *in vivo* have not yet been elucidated. To identify the PKCγ substrates involved in dopamine release, we used PKCγ-KO mice and a phosphoproteome analysis. We found 10 candidate phosphoproteins that had decreased phosphorylation levels in the striatum of PKCγ-KO mice. We focused on Pak-interacting exchange factor-β (βPIX), a Cdc42/Rac1 guanine nucleotide exchange factor, and found that PKCγ directly phosphorylates βPIX at Ser583 and indirectly at Ser340 in cells. Furthermore, we found that PKC phosphorylated βPIX *in vivo*. Classical PKC inhibitors and βPIX knock-down (KD) significantly suppressed Ca^{2+}-evoked dopamine release in PC12 cells. Wild-type βPIX, and not the βPIX mutants Ser340 Ala or Ser583 Ala, fully rescued the decreased dopamine release by βPIX KD. Double KD of Cdc42 and Rac1 decreased dopamine release from PC12 cells. These findings indicate that the phosphorylation of βPIX at Ser340 and Ser583 has pivotal roles in Ca^{2+}-evoked dopamine release in the striatum. Therefore, we propose that PKCγ positively modulates dopamine release through β2PIX phosphorylation. The PKCγ-βPIX-Cdc42/Rac1 phosphorylation axis may provide a new therapeutic target for the treatment of parkinsonian syndrome.

Key words: βPIX; Cdc42; dopamine; Parkinson's disease; phosphoproteome; PKC

Introduction

Protein kinase C (PKC) is an important kinase in the enhancement of Ca^{2+}-triggered exocytosis (Iwasaki et al., 2000; Barclay et al., 2003). The PKC family consists of at least 10 subtypes and is divided into the following three subfamilies: conventional PKC (cPKC), novel PKC, and atypical PKC (Nishizuka, 1988, 1992). Among PKCs, only cPKCs (including PKCγ, which is a neuron-specific PKC isoform; Saito and Shirai, 2002) are activated by Ca^{2+} because they contain a C2 domain that specifically binds to Ca^{2+} and phosphatidylserine (PS; Murray and Honig, 2002).

Received Oct. 6, 2013; revised May 18, 2014; accepted May 29, 2014.

Author contributions: N. Saito designed research; T.S., H.T., N.A., Y.A., K.K., T.N., and N.H. performed research; K.Y. contributed unpublished reagents/analytic tools; T.U., T.M., T.T., N. Sakai, and N. Saito analyzed data; T.S., T.U., and N. Saito wrote the paper.

We thank Sumio Sugano (University of Tokyo) and Yoshihide Hayashizaki (RIKEN Omics Science Center and Research Association for Biotechnology) for kindly providing the βPIX cDNA and Hiroshi Kiyonari and Kazuki Nakao (RIKEN CDB) for mice preservation.

The authors declare no competing financial interests.

Correspondence should be addressed to Naoaki Saito, 1-1 Rokkodai-cho, Nada-ku, Kobe 657-8501 Japan. E-mail: naosaito@kobe-u.ac.jp.

DOI:10.1523/JNEUROSCI.4278-13.2014

 0270-6474/14/349268-13$15.00/0

The AS/AGU rat, a spontaneously occurring mutated animal that exhibits locomotor abnormalities, progressive dopaminergic (DAergic) neuronal degeneration in the substantia nigra (SN), and lower extracellular levels of dopamine (DA) in the striatum, has been used as a valuable model for parkinsonian syndrome (Payne et al., 2000). It is noteworthy that a mutation in PKCγ that leads to the early termination at the C2 domain without possessing the catalytic domain causes parkinsonian syndrome in AS/AGU rats (Craig et al., 2001). The mutation in AS/AGU rats should result in the kinase-dead form of PKCγ, but it is still unclear how the mutation causes parkinsonian symptoms.

PKC has been shown to modify exocytosis in at least three steps: (1) increased vesicle recruitment into readily releasable pools (Gillis et al., 1996; Stevens and Sullivan, 1998), (2) acceleration of fusion pore expansion (Scepek et al., 1998), and (3) changes in the kinetics of exocytosis (Graham et al., 2002). However, only the functional consequences of the phosphorylation of SNAP25 (Iwasaki et al., 2000), synaptotagmin I (Hilfiker et al., 1999), and Munc18 (Barclay et al., 2003) by PKC have been established on exocytosis *in vivo*. Furthermore, no attempts have been made to achieve a comprehensive understanding of DA exocytosis through an identification of

PKCγ substrates. Therefore, we attempted to identify the PKC substrates involved in exocytosis to reveal the mechanisms of regulated exocytosis.

Pak-interacting exchange factor-β (βPIX) is a Rho guanine nucleotide exchange factor (GEF) that specifically activates Rac1 and Cdc42 (Shin et al., 2002; Shin et al., 2004; Chahdi et al., 2005; Feng et al., 2006; Shin et al., 2006; ten Klooster et al., 2006; Chahdi and Sorokin, 2008). βPIX has been reported to be an essential element of the exocytotic machinery in neuroendocrine cells (Audebert et al., 2004; Momboisse et al., 2009). To date, there have been several studies on βPIX phosphorylation (Shin et al., 2002; Chahdi et al., 2005; Shin et al., 2006; Mayhew et al., 2007), but there have been no reports of the involvement of βPIX phosphorylation in DA release.

In the present study, we found that the AS/AGU rat is indeed a PKCγ-knock-out (KO) animal, and our phosphoproteome analysis using PKCγ KO mice found 10 candidates in the striatum that are phosphorylated by PKCγ. Among the 10 candidates, we demonstrated that PKCγ activated DA release through the phosphorylation of βPIX.

Materials and Methods

Antibodies. The anti-GFP antibody (Ab) and the anti-vesicular monoamine transporter 2 (VMAT2) Ab recognizing the C-terminal of mouse VMAT2 were prepared in house. The anti-PKCγ (C2-domain) monoclonal Abs specifically recognizing C2-domain of PKCγ have been described previously (Kose et al., 1990). The following Abs were purchased: anti-FLAG from Sigma-Aldrich (catalog #P2983 RRID:AB_439685); anti-βPIX (SH3 domain) from Millipore; anti-β-actin (catalog #ab66338 RRID:AB_2289239) and anti-PKCγ (N-terminal) specifically recognizing N-terminal of PKCγ from Abcam; anti-glutathione S-transferase (GST) (catalog #sc-33613 RRID:AB_647588), anti-PKCα (catalog #sc-208 RRID:AB_2168668), anti-PKCβ1 (catalog #sc-209 RRID:AB_2168968), anti-PKCβ2 (catalog #sc-210 RRID:AB_2252825), and anti-PKCγ (catalog #sc-211 RRID:AB_632234) from Santa Cruz Biotechnology; and anti-serPKC motif (catalog #2261S RRID: AB_330310), anti-βPIX (catalog #4515S RRID:AB_2274365) for immunoprecipitation (IP), and anti-postsynaptic density-95 (PSD95; catalog #2507S RRID:AB_10695259) from Cell Signaling Technology.

Production of anti-phosphoThr76, anti-phosphoSer340, anti-phosphoSer583, and anti-β2PIX Abs. The production of anti-phospho Abs was performed as described previously (Matsubara et al., 2012). For the preparation of anti-phospho-Thr76 (pT76), anti-phospho-Ser340 (pS340), and anti-phospho-Ser583 (pS583) βPIX Abs, oligopeptides corresponding to the amino acids of human βPIX containing pT76 [VSPKSG(pT)LKSPP], pS340 [SASPRM(pS)GFIYQ], and pS583 [SLGRRS(pS)LSRLE] were used as antigens, respectively. After the fifth boost, serum was collected and purified with an affinity column and the non-phospho-antigen peptide. The anti-β2PIX Ab was obtained by eluting the IgG from those that were bound to the nonphospho-Ser583 peptide column.

Animals. The AS/AGU rats were provided by R.W. Davies (Payne et al., 2000). The PKCγ-Cre knockin (KI) mouse was provided by Z.F. Chen (Ding et al., 2005). After the sixth backcross, homozygous littermates obtained by crossing the heterozygous PKCγ-Cre KI mouse were used as the PKCγ KO and wild-type (WT) mice in the studies. All animal studies were approved by the Institutional Animal Care and Use Committee and conducted according to the Kobe University Animal Experimentation Regulations.

Sample preparation and Western blot analysis. The brains from AS/AGU rats and mice were homogenized and the concentrations of the proteins were measured with a bicinchoninic acid (BCA) protein assay kit (Thermo Fisher Scientific). SDS-PAGE and immunoblot analyses were performed as described previously (Adachi et al., 2005).

Preparation of P2 synaptosomal fraction. Adult male mouse brains were collected and homogenized in ice-cold 0.32 M sucrose solution containing 1 mM phenylmethylsulfonyl fluoride, 20 μg/ml leupeptin, and a phosphatase-inhibitor cocktail (Nacalai Tesque). The total homogenate was subjected to centrifugation at 800 × *g* for 12 min at 4°C to remove the nuclei and the supernatant, which we defined as the total fraction, was further centrifuged at high speed at 22,000 × *g* for 20 min at 4°C. The pellet was used as the P2 synaptosomal fraction. To determine the efficiency of the P2 synaptosomal extraction process, we compared the amount of VMAT2 and PSD95 proteins between the total fraction and P2 synaptosomal fraction in the same amount of protein (50 μg), which was calculated using the BCA protein assay kit.

In vivo *microdialysis. In vivo* microdialysis was performed with male mice essentially as described previously (Koda et al., 2010; Ago et al., 2013). In brief, mice were anesthetized by injection of sodium pentobarbital (40 mg/kg, i.p.), and a guide cannula (one site per animal) for a dialysis probe (Eicom) was implanted stereotaxically in the dorsal striatum (anterior 0.1 mm, lateral 1.8 mm, ventral 2.2 mm relative to the bregma and skull; Franklin and Paxinos, 1997). The cannula was cemented in place with dental acrylic and the animals were maintained warm and allowed to recover from anesthesia. The active probe membrane was 1 mm in length. Two days after the surgery, the probe was perfused with Ringer's solution (147.2 mM NaCl, 4.0 mM KCl, and 2.2 mM $CaCl_2$, pH 6.0; Fuso Pharmaceutical Industries) at a constant flow rate of 1 μl/min. To prepare the Ringer's solution containing 100 mM K^+, an identical amount of sodium was replaced for maintaining isoosmolarity. Experiments were initiated after a stabilization period of 3 h. Microdialysis samples (20 μl) were collected every 20 min and were assayed for DA by high-performance liquid chromatography (HPLC) with electrochemical detection. No-net-flux microdialysis experiments were conducted in a PKCγ KO and WT mice as described previously (Justice, 1993; Chefer et al., 2005; Hewett et al., 2010). Three different concentrations of DA in Ringer's solution (C_{in} of 0, 5 and 20 nM DA) were perfused through the probe and DA in the perfusates (C_{out}) was measured in the fifth fraction following 4 fractions (equilibration period) at each applied DA concentration. A slope was calculated for the linear regression for DA applied (C_{in}) and the difference between dopamine applied and DA measured ($C_{in} - C_{out}$). The slope (extraction fraction) is an indirect measure of dopamine transporter (DAT) dynamics *in vivo* to remove extracellular DA.

Measurement of DA and DA metabolite levels in striatum. The concentrations of DA were quantified by HPLC with an electrochemical detector (ECD-100; Eicom; Kawasaki et al., 2006; Kawasaki et al., 2007). Tissue samples were homogenized in 0.2 M perchloric acid containing 100 μM EDTA and isoproterenol as an internal standard. The homogenate was centrifuged at 15,000 × *g* for 15 min at 0°C. The supernatant was filtered through a 0.22 μm membrane filter (Millipore), and then a 10 μl aliquot of the sample was injected onto the HPLC column every 30 min for the DA assay. An Eicompak SC-5ODS column (3.0 mm i.d. × 150 mm; Eicom) was used, and the potential of the graphite electrode (Eicom) was set to +750 mV against an Ag/AgCl reference electrode. The mobile phase contained 0.1 M sodium acetate/0.1 M citrate buffer, pH 3.5, 190 mg/L octanesulfonic acid, 5 mg/L EDTA, and 17% (v/v) methanol. Data were calculated by analyzing the peak area of the external standard of dopamine hydrochloride (Sigma-Aldrich).

Cell culture. COS7 and HEK293 cells were cultured in DMEM and Eagle's minimum essential medium (Nacalai Tesque), respectively, which were supplemented with 10% fetal bovine serum, penicillin (100 units/ml), and streptomycin (100 μg/ml). Nonessential amino acids (100 μM) were added for HEK293 cells. PC12 cells were cultured in DMEM containing 10% fetal bovine serum and 5% horse serum. All cells were cultured at 37°C in a humidified atmosphere containing 5% CO_2.

Construction of plasmids. WT PKCγ was cloned into pcDNA3.1 (Life Technologies) and the subdomains of PKCγ were cloned into pcDNA3.1 with GFP, as described previously (Seki et al., 2005). Human βPIX was provided by the RIKEN BioResource Center through the National BioResource Project of MEXT in Ibaraki, Japan (Ota et al., 2004). For the construction of plasmids encoding full-length β2PIX that was fused with 3xFLAG at the N terminal, β2PIX with a NotI/BamHI site that was produced by PCR was cloned into a 3xpFLAG-CMV10 vector (Sigma-Aldrich). Because the target sequence for rat βPIX knock-down (KD; sh369) was located in the coding region of βPIX, sh369-resistant β2PIX in the 3xpFLAG-CMV10 vector was made by placing 6-base silent

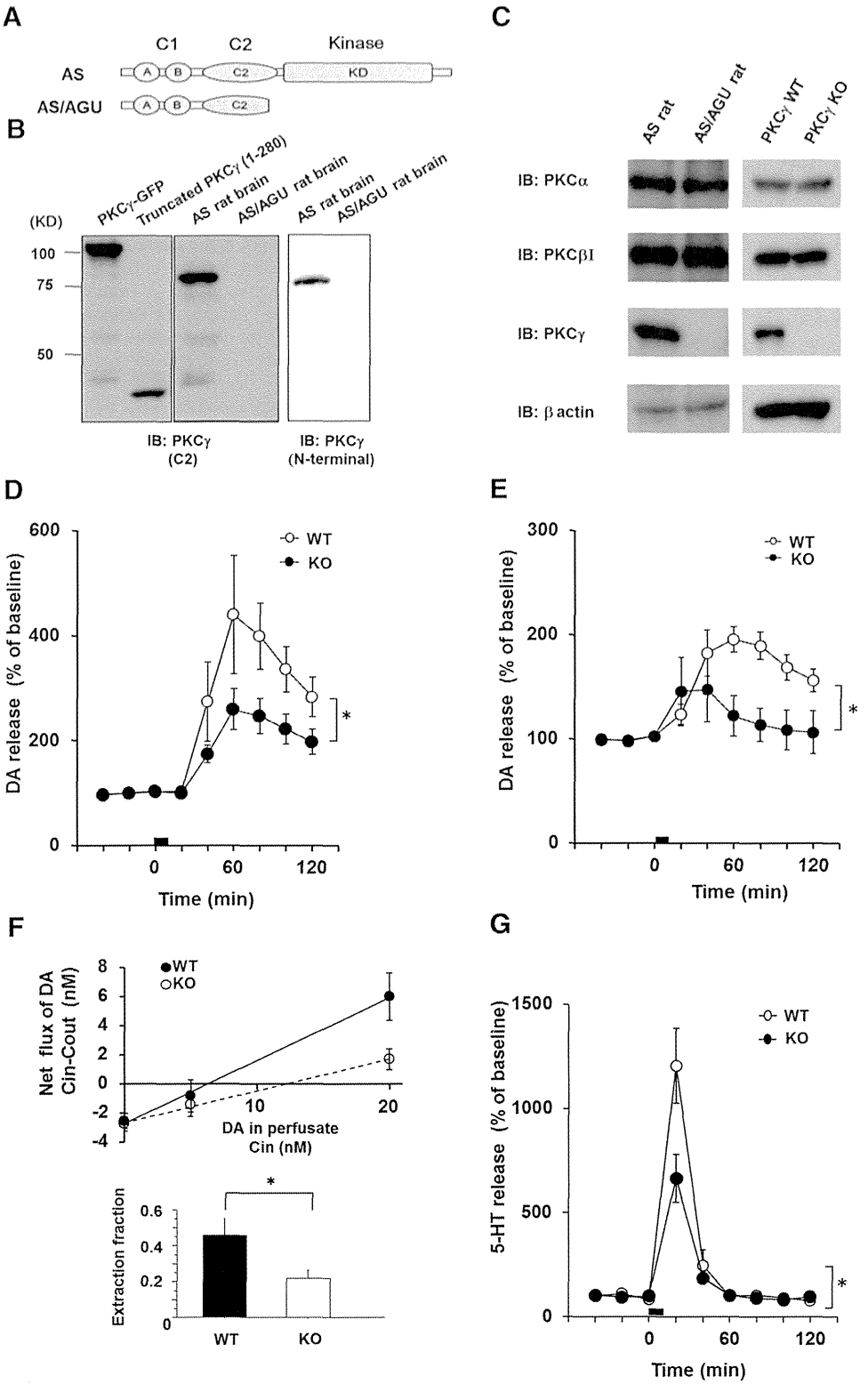

Figure 1. The PKCγ KO model exhibits symptoms of parkinsonian syndrome. ***A***, Schematic illustrations of the PKCγ protein and AS/AGU mutations. The truncated PKCγ polypeptide terminates within the C2 domain. ***B***, Recombinant truncated PKCγ (1–280 aa), which was transfected in COS-7 cells, the AS rat brain lysate, and the AS/AGU rat brain lysate, was detected by immunoblot analysis with an anti-PKCγ (C2-domain) monoclonal antibody and anti-PKCγ (N terminal) antibody, respectively. ***C***, The PKCγ KO was confirmed by immunoblot analysis of the whole brain of the AS/AGU rats and PKCγ KO mice. Arrowheads are recombinant PKCγ-GFP and PKCγ (1–280aa)-GFP, which were used as positive controls. ***D***, *In vivo* microdialysis in the striatum of the PKCγ KO mice. A high level of K^+ was perfused into the striatum through a dialysis probe for the time indicated by the square at 3–4 months. The results are expressed as mean ± SEM ($n = 4–5$, interaction of the genotype and time for DA release that was stimulated by high K^+ levels; $^*p < 0.05$, $F_{(8,48)} = 2.31$, repeated two-way ANOVA). ***E***, *In vivo* microdialysis for DA in the striatum of the PKCγ-KO (KO) mice that were stimulated with METH. METH (1 mg/kg) was perfused into the striatum through a dialysis probe for the time indicated by the square at 3 months (*Figure legend continues.*)

changes within the targeting sequence (5′-CAaACgAGtGAaAAaTTa-3′) with a QuikChange Multisite-Directed Mutagenesis Kit (Agilent Technologies). For construction of plasmids encoding full-length β2PIX or fragments that were fused to GST, full-length β2PIX and the SH3 (1–92 aa), DH (93–274 aa), and PH (275–400 aa) C-terminal (401–625 aa) regions were amplified by PCR with a Not1/BamH1 site and cloned into the pGEX-6P1 vector. Substitutions of Ser or Thr to Ala or Glu at the identified phosphorylation sites (Thr76Ala, Ser215Ala, Ser340Ala or Glu, and Ser583Ala or Glu) were introduced with a QuikChange kit.

Protein expression. Protein expression was performed as described previously (Kawasaki et al., 2010). In brief, BL21 pLys *Escherichia coli* and Sf9 cells were transformed with expression plasmids. *E. coli* and Sf9 cells were harvested and lysed. For the purification of recombinant proteins, GST-fusion proteins were purified with glutathione-Sepharose 4B resin (GE Healthcare Biosciences).

RNAi: short hairpin RNA and small interfering RNA. Double-stranded oligonucleotides were cloned into the short hairpin RNA (shRNA) expression vector, pSuper (puro; Oligoengine). The target sequence for the shRNA rat βPIX KD was 5′-GCAGACCAGCGAGAAGTTGAG-3′ (sh369; cording nucleotides 369–389). Because the βPIX shRNA sequence that we used was common to both the β1 and β2 isoforms, KDs of both β1 and β2 in PC12 cells were examined with βPIX SH3- and β2-specific antibodies. The synthesized small interfering RNA (siRNA) for rat βPIX was composed of a mixture of 4 oligonucleotides (si878: 5′-GGGAUGACAUAAAGACGUU-3′, si806: 5′-AGUGUCAAGAAGU ACGAAA-3′, si1115: 5′-GGAGCAUGAUCGAGCGCAU-3′, and si1153: 5′-CAACAGGACUUGCACGAAU-3′) was purchased from Thermo Fisher Scientific (SmartPool). Verified shRNA plasmids for KD of Cdc42 (sh197; 5′-GATTACGACCGCTGAGTTA-3′; Ueyama et al., 2014) and Rac1 (sh618; 5′-CCTTTGTACGCTTTGCTCA-3′; Ueyama et al., 2006) were described previously.

In vitro *PKC phosphorylation assay.* An *in vitro* PKC phosphorylation assay was performed as described previously (Kawasaki et al., 2010). In brief, precipitated FLAG-tagged β2PIX proteins or purified GST-tagged β2PIX were incubated with 200 ng of GST-tagged PKCγ or GST and the following buffers: 20 mM Tris, pH 7.4, 0.5 mM $CaCl_2$, 10 μM ATP, 0.5 mCi [γ-^{32}P] ATP, 8 μg/ml PS, and 0.8 μg/ml (±)-1,2-didecanoylglycerol (DO) in a 50 μl final volume. The samples were incubated with or without PKC inhibitors, including GF109203X (GFX), which was used as a pan PKC inhibitor, and Gö6976, which was used as a cPKC inhibitor, at 30°C for 15 min. For the calculation of the relative phosphorylation levels, the densitometries of the autoradiography were normalized with the total protein levels. The average relative phosphorylation levels of PKCγ stimulation were defined as 1.00.

PKC phosphorylation assay in cells. A PKC phosphorylation assay in cells was performed as described previously (Kawasaki et al., 2010) but with slight modifications. In brief, HEK293 cells were transfected with WT β2PIX in 3xpFLAG-CMV10 with a NEPA21 electroporator (Nepa Gene). After 12-O-tetradecanoylphorbol 13-acetate (TPA) stimulation with or without PKC inhibitors for 30 min in HEPES buffer at 37°C, the cells were collected and resuspended in homogenization buffer containing 150 mM NaCl, 10 mM ethylene glycol tetraacetic acid, 2 mM ethylenediamine tetracetic acid, 10 mM HEPES, pH 7.4, 1 mM phenylmethylsulfonyl fluoride, 20 μg/ml leupeptin, and a phosphatase-inhibitor cocktail. The precipitated proteins were separated by SDS-PAGE. The phosphorylated proteins were visualized with phospho-Abs. For the calculation of the relative phosphorylation levels, the densitometries of the immunoblots of the phospho-Abs were normalized to the total protein levels in each experiment and the averages of the relative levels of phosphorylation in more than three independent experiments are presented. The phosphorylation levels of the prestimulations were defined as 1.00.

PKC phosphorylation assay in vivo. The mice P2 synaptosomal fraction was resuspended in HEPES buffer containing 1 mM phenylmethylsulfonyl fluoride, 20 μg/ml leupeptin, and a phosphatase-inhibitor mixture and used for the *in vivo* PKC phosphorylation assay (Wu et al., 1982). After 2 μM TPA stimulation with or without 2 μM GFX for 30 min in HEPES buffer at 37°C, the P2 fraction was collected and resuspended in homogenization buffer containing 150 mM NaCl, 10 mM ethylene glycol tetraacetic acid, 2 mM ethylenediamine tetracetic acid, 10 mM HEPES, pH 7.4, 1 mM phenylmethylsulfonyl fluoride, 20 μg/ml leupeptin, and the phosphatase-inhibitor mixture. The precipitated proteins were separated by SDS-PAGE. The phosphorylated proteins were visualized with ser-PKC motif Abs.

DA release assay. DA release assays in βPIX KD cells were performed 96 h after transfection by NEPA21. PC12 cells were washed thrice with 500 μl of incubation solution (140 mM NaCl, 5 mM KCl, 2 mM $CaCl_2$, 1 mM $MgCl_2$, 2 mM glucose, 20 μM pargyline, and 10 mM HEPES, pH 7.5) and then incubated for 60 min in 500 μl of incubation solution with ^{3}H-DA (PerkinElmer), followed by three washes with 500 μl of incubation solution. The cells were allowed to rest or were stimulated with 500 μl of a high-K^+ solution containing 100 mM KCl and 35 mM NaCl for 10 min. The supernatant was collected and the cells were harvested in 500 μl of incubation solution with 2% Triton X-100. The amount of DA that was secreted into the medium and retained in the cells was measured in 500 μl of samples with a scintillation counter LS-6500 (Beckman Coulter). DA secretion was expressed by the following formula: %DA = (^{3}H in supernatant)/(^{3}H in supernatant + ^{3}H in cell lysate). A collagen-IV-coated six-well plate (BD Biosciences) was used for the DA release assay.

Mass spectrometry for β2PIX-phosphorylation site identification. Mass spectrometry for β2PIX-phosphorylation site identification was performed as described previously (Sakuma et al., 2012). After the *in vitro* PKC phosphorylation assay and electrophoresis, silver-stained bands that corresponded to GST-tagged β2PIX proteins were excised and destained. After reduction-alkylation reactions, the proteins in the gels were digested with porcine trypsin (sequencing grade; Promega) in 50 mM ammonium bicarbonate for 15 h at 37°C. The peptide fragments extracted from the gels were subjected to liquid chromatography/tandem mass spectrometry (LC/MS/MS) with a high-performance liquid chromatography system (Paradigm MS4; Michrom Bioresources) coupled to a linear ion trap mass spectrometer (Finnigan LTQ Orbitrap XL; Thermo Fisher Scientific). The LC/MS/MS data were interpreted with a MASCOT MS/MS ions search (Matrix Science).

Phosphoproteome analysis. Phosphoproteome analysis was performed as described previously with some modifications (Saito et al., 2006). Mice striata were dissolved in 50 mM Tris HCl, pH 9.0, 8 M urea, 10 mM ethylenediamine tetracetic acid, 1 mM phenylmethylsulfonyl fluoride, 20 μg/ml leupeptin, and a phosphatase inhibitor mixture. After homogenization with a Dounce homogenizer (10 strokes), the resultant solution was centrifuged at 2000 × *g* for 5 min and the supernatant was collected. The protein amounts were measured with a BCA protein assay kit. The proteins from the striatum were dried and resuspended in 50 mM Tris HCl buffer, pH 9.0, containing 8 M urea at a concentration of 10 μg/μl. These mixtures were subsequently reduced with dithiothreitol, alkylated with acrylamide, and digested with Lys-C endopeptidase at 37°C overnight, followed by trypsin digestion at 37°C overnight. The digested solutions were desalted and concentrated with Empore high-performance extraction disk cartridges (3M). Phosphopeptide enrichment was performed with hydroxy acid-modified metal oxide chromatography (HAMMOC; Titansphere Phos-TiO Kit; GL Sciences; Kyono et al., 2008). For elution of the phosphopeptides, 50 μl of 5% NH_3 and 5% pyrrolidine were used. The fractions were immediately acidified and desalted with SPE-C tips (GL Sciences). A Tomy CC-105 vacuum evap-

←

(Figure legend continued.) ($n = 4$, interaction of the genotype and time for DA release stimulated by METH, $F_{(8,48)} = 3.37$; $^*p < 0.01$, repeated two-way ANOVA). ***F***, No-net flux microdialysis to quantitate basal DAT activity in PKCγ KO mice. Three different concentrations of DA in CSF (0, 5, and 20 nM DA) were perfused through the probes to determine the extracellular DA concentration and extraction fraction. Linear regression for the DA perfused and DA measured provided extraction fraction (slope) as an indirect measure of DAT activity *in vivo* to remove extracellular DA. Extraction fraction for WT and KO mice are shown. Data represent mean ± SEM ($n = 4$ and 5 for WT and KO mice, respectively, $^*p < 0.05$). ***G***, *In vivo* microdialysis of serotonin in the striatum of the PKCγ-KO mice that were stimulated by high K^+ levels. K^+ (100 mM) was perfused into the striatum through a dialysis probe for the time indicated by the square at 3–4 months. The results are expressed as mean ± SEM ($n = 4$, interaction of the genotype and time for serotonin release that was stimulated by high K^+ levels, $F_{(8,48)} = 5.399$; $^*p < 0.001$, repeated two-way ANOVA).

Table 1. DA and DA metabolite levels in the striatum of PKCγ WT and KO mice

Age (mo)	Genotype	DA (ng/g weight)	DOPAC (ng/g weight)	HVA (ng/g weight)
3	KO	19629.5 ± 625.4	1838.6 ± 68.9	1490.6 ± 89.0
	WT	19516.4 ± 361.1	1999.1 ± 103.4	1652.1 ± 18.4
6	KO	20667.2 ± 803.5	1671.2 ± 113.0	1620.0 ± 93.9
	WT	17416.8 ± 781.3	1559.2 ± 77.2	1334.6 ± 63.7
12	KO	28911.0 ± 1801.4	2576.0 ± 277.9	2378.1 ± 161.3
	WT	29564.9 ± 2581.4	2253.1 ± 202.2	2392.2 ± 128.4

Results are expressed as mean ± SEM of 4–5 mice.

HVA, Homovanillic acid.

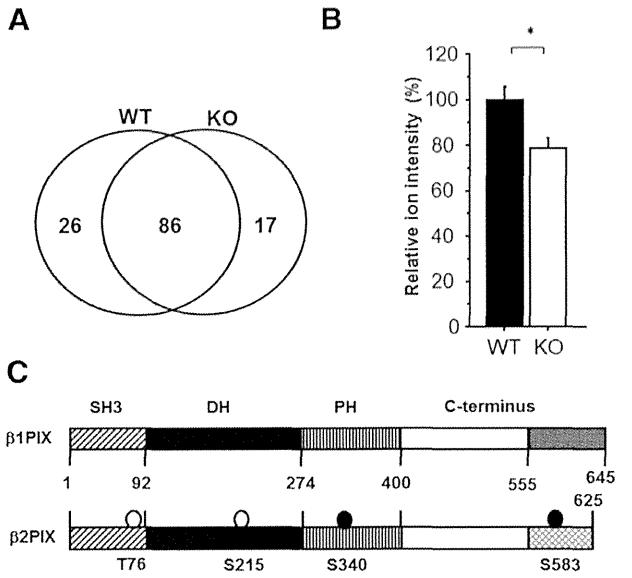

Figure 2. Phosphoproteome analysis revealed 10 phosphopeptides with decreased average ion intensity in PKCγ KO mice striatum. ***A***, Overview of the phosphoproteome (WT, $n = 5$; KO, $n = 4$). ***B***, Average ion intensity of the Ser340 βPIX phosphopeptide is calculated in both PKCγ KO and WT mice ($n = 4–5$; $^*p < 0.05$, unpaired t test). The relative average ion intensity of WT mice was defined as 100%. The results are expressed as mean ± SEM. ***C***, Schematic illustrations of the β1 and β2 PIX protein. The phosphorylation sites that were determined by the *in vitro* PKC phosphorylation assay and the phosphoproteome analysis are circled. The open circles are the phosphorylation sites that were determined only *in vitro*. The closed circles are the phosphorylation sites that were determined *in vitro* and *in vivo*.

orator was used to concentrate the sample and the phosphopeptides were analyzed by LC/MS/MS.

Statistical analysis. The data are presented as mean ± SEM and were analyzed with unpaired t tests, one-way ANOVA with a *post hoc* Dunnett's test, or a repeated two-way ANOVA. The statistical analyses were performed with the Statview 5.0J software package (SAS Institute). p-values of 5% or less were considered statistically significant.

Results

PKCγ KO animals exhibited parkinsonian symptoms, including DA release impairment in the striatum

AS/AGU rats show altered behaviors (Craig et al., 2001), DA release impairment, and the pathology of the nigrostriatal system resembles the pathology observed in human patients with parkinsonian syndrome (Campbell et al., 1996; Payne et al., 2000). AS/AGU rats have a spontaneously occurring mutation that changes the CAG (Glu281) codon to a TAG (stop codon) in PKCγ, and the putatively truncated PKCγ, if produced, will terminate at the fifth residue from the C terminus of the last strand of the β-sheet structure of the C2 domain (Fig. 1*A*). The truncated protein may result in a severe or complete loss of the kinase function of PKCγ, although it has not yet been clarified whether the truncated protein is expressed in AS/AGU rats. Although both anti-PKCγ (N terminal) Ab and anti-PKCγ (C2-domain) Ab detected an 80 kDa single band in AS rats, no band was detected in the AS/AGU rats (Fig. 1*B*). These findings indicated that PKCγ was not expressed in AS/AGU rats, suggesting the hypothesis that PKCγ KO mice show similar symptoms as those observed in AS/AGU rats. We first confirmed that our PKCγ KO mice did not express PKCγ, whereas the expression levels of other members of cPKCs were unaltered (Fig. 1*C*). To determine the effects of the PKCγ KO on DA release in the striatum, we performed *in vivo* microdialysis in the striatum. The basal line extracellular levels of DA in the striatum did not differ significantly between the PKCγ WT and KO mice. After treatment with high levels of K^+ (Fig. 1*D*) and methamphetamine (METH; Fig. 1*E*), the increase in DA release in the WT was significantly larger than that in the KO 3–4 months after birth. Although high K^+ levels induced DA release is mediated by exocytosis and not by DAT, PKC induces DAT endocytosis (Daniels and Amara, 1999), which may decrease the extracellular DA levels by increasing

Table 2. List of phosphopeptides with a PKC phosphorylation motif

Protein name	Accession no.	Sequence	Site	No. of phosphopeptides		Lowest peptide score		Highest peptide score		Average ion intensity		
				WT	KO	WT	KO	WT	KO	WT	KO	WT/KO
Gap junction alpha-1 protein	NP 034418	KVAAGHELQPLAIVDQRPSSRA	S365	7	0	11	—	28	—	3	0.4	7.3
Disks large-associated protein 1	NP 808307	RSLDSLDPAGLLTSPKF	S437	5	0	48	—	77	—	3.4	0.8	4.4
MAP kinase-activating death domain protein	NP 001171190	RATLSDSEIETNSATSAIFGKA	T1235	8	4	40	26	90	58	3.7	1	3.9
DnaJ homolog subfamily C member 5	NP 001258513	RSLSTSGESLYHVLGLDKN	S10	54	55	3	4	88	85	969	299.5	3.2
Calnexin	NP 001103969	KAEEDEILNRSPRN	S582	6	2	25	22	31	34	3.1	1.8	1.8
Stathmin	NP 062615	KRASGQAFELILSPRS	S16	26	23	8	6	93	84	12.1	7.5	1.6
Stathmin	NP 062615	RASGQAFELILSPRS	S25	25	17	5	19	81	83	7.4	5.9	1.3
Rho guanine nucleotide exchange factor 7	NP 001106989	RMSGFIYQGKL	S340	3	0	24	—	59	—	1.8	1.4	1.4
Reticulon-4	NP 077188	RRGSGSVDETLFALPAASEPVIPSSAEKI	S165	15	8	34	41	70	59	2.3	1.7	1.3
α-adducin	NP 001019629	KFRTPSFLKK	S724	3	2	7	9	29	25	6.1	4.8	1.3
β-adducin	NP 001258786	KDIATEKPGSPVKS	S594	10	8	10	17	50	56	0.4	0.3	1.2

Phosphopeptides with a WT/KO ratio >1.0 are listed. The numbers of phosphorylation sites are based on the results of mice in PhosphoSitePlus (www.phosphosite.org). S and T are the identified phosphorylation sites. Number of phosphopeptides means the total numbers of the phosphopeptides in each group ($n = 4$). Highest or lowest peptide score means the highest or lowest peptide score in each group ($n = 4$). Peptides that were not detected are shown as —.

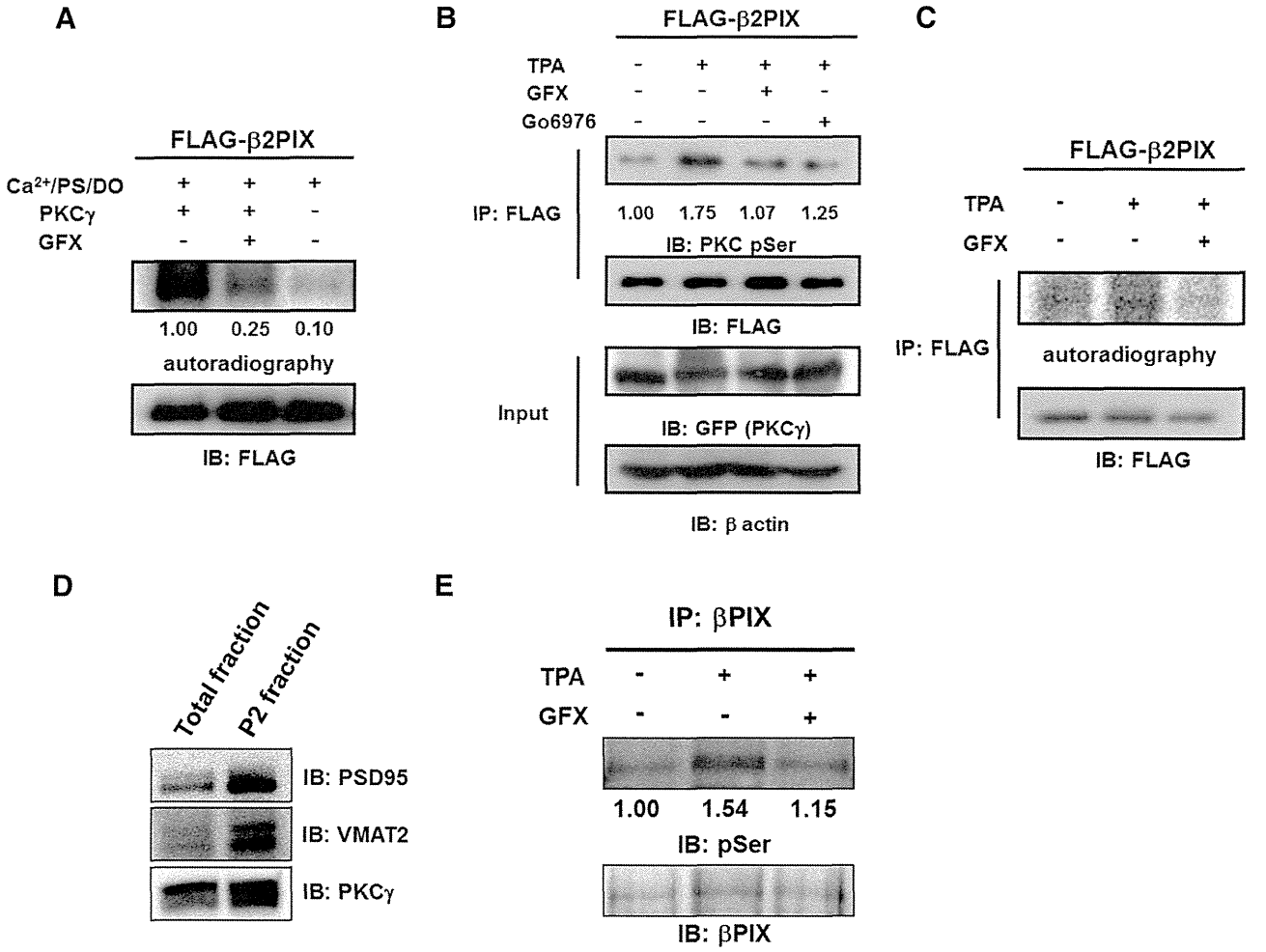

Figure 3. βPIX is phosphorylated by PKCγ *in vitro*, in cells, and *in vivo*. ***A***, *In vitro* phosphorylation of β2PIX. FLAG-tagged β2PIX proteins were purified and incubated with or without recombinant PKCγ in the presence of PKC activator (PS/DO/Ca^{2+}) and [γ-^{32}P] ATP for 20 min. The *in vitro* phosphorylation of β2PIX was also performed in the presence of GFX. The phosphorylated proteins were detected by autoradiography and the levels of protein expression were determined by Western blotting with an anti-FLAG antibody. The numbers show the relative phosphorylation levels that were normalized to PKCγ stimulation as 1.00 ($n = 3$). ***B***, In-cell phosphorylation of β2PIX. HEK293 cells expressing FLAG-tagged β2PIX and GFP-tagged PKCγ were stimulated with 1 μM 12-O-TPA for 20 min in the presence or absence of 1 μM GFX or 1 μM Gö6976. FLAG-tagged β2PIX proteins were purified with anti-FLAG agarose resin. Phosphorylated proteins were detected by an immunoblot analysis with an anti-pSer PKC motif antibody. Protein expression was determined by Western blotting with an anti-FLAG antibody. The average relative phosphorylation levels for each experimental condition were normalized to the prestimulation signal set as 1.00 ($n = 5$). ***C***, PC12 cells expressing FLAG-tagged β2PIX were incubated with ^{32}P monosodium phosphate and stimulated with 1 μM 12-O-TPA in the absence or presence of 1 μM GFX. FLAG-tagged β2PIX proteins were purified with anti-FLAG agarose resin. Phosphorylated proteins were detected by autoradiography, and protein expression was determined by immunoblots with an anti-FLAG antibody. ***D***, The same amount of samples of total fraction and the P2 synaptosomal fraction were immunoblotted by anti-PSD95 antibody as a postsynaptic marker, anti-VMAT2 antibody as a presynaptic marker, and anti-PKCγ antibody. ***E***, the P2 synaptosomal fraction was stimulated with 2 μM 12-O-TPA in the absence or presence of 2 μM GFX. βPIX proteins were purified with anti-βPIX antibody. Phosphorylated proteins were detected by phospho-Abs. The numbers show the relative phosphorylation levels that were normalized to pretreatment as 1.00 ($n = 3$).

DAT activity in PKCγ KO mice striatum. To evaluate the DAT activity in PKCγ KO mice, we performed the no-net-flux microdialysis experiment. The slope (extraction fraction) is the measure of the activity of DAT *in vivo*. Fig. 1*G* shows decreased DAT activity in the striatum of PKCγ KO mice, suggesting that PKCγ KO mice tend to have increased rather than decreased extracellular DA levels compared with WT mice (Fig. 1*F*). Consistent with our results, the increase in the serotonin release stimulated by high K^+ levels in WT was also significantly larger than that of the KO (Fig. 1*G*), as described previously in AS/AGU rats (Al-Fayez et al., 2005). Because we had preliminary data that suggested slight loss of DAergic neurons in 12-month-old, but not 3- or 6-month-old, PKCγ KO mice, there was a possibility that the decrease in DA release in PKCγ KO mice was due to the decrease in DA in the striatum. We measured DA and its metabolites using HPLC in the striatum. No difference in DA or DA metabolite levels in the striatum was observed between PKCγ KO mice and WT mice at 3, 6, and 12 months (Table 1), suggesting that DA release disorder was from the exocytotic machinery disorder instead of the lack of the DAergic neurons in the nigrostriatum system. These results suggested that the PKCγ KO mice would show similar parkinsonian symptoms as those observed in the AS/AGU rats. From the analysis of the PKCγ KO mice and AS/AGU rats, we concluded that PKCγ KO animals could be used as a practical model of parkinsonian syndrome.

Phosphoproteome analysis identified 10 phosphoproteins, including βPIX, with a PKC-phosphorylation motif

We hypothesized that a loss or decrease of PKCγ-mediated phosphorylation in the nigrostriatal system results in DA release im-